

Supporting Information for:

Cooperative silanetriolate-carboxylate sensitiser anchoring for outstanding stability and improved performance of dye-sensitised photoelectrodes

Maxime Fournier,^{†*} Dijon A. Hoogeveen,[‡] Shannon A. Bonke,^{†§} Leone Spiccia,[‡] and
Alexandr N. Simonov^{†*}

[†] School of Chemistry and ARC Centre of Excellence for Electromaterials Science, Monash University,
Victoria 3800, Australia

[§] Institut Nanospektroskopie, Helmholtz-Zentrum Berlin für Materialien und Energie, Kekuléstraße 5, 12489 Berlin,
Germany

E-mail: maxime.fournier@monash.edu (M.F.), alexandr.simonov@monash.edu (A.N.S.)

TABLE OF CONTENTS

	Page
Nomenclature Discussion	S3
Table S1. Structures and nomenclature of anchoring groups	S3
Scheme S1. Synthesis of RuAc.2PF₆	S4
Scheme S2. Synthesis of RuAc.2Cl.2H₂O	S5
Scheme S3. Synthesis of RuP.2Cl	S6
Peptide coupling synthesis methodology	S7
Scheme S4. Synthesis of RuNPhSiSi.2PF₆	S8
Scheme S5. Synthesis of RuNPhAcSi.2Cl	S9
Scheme S6. Synthesis of RuNPhAcAc.2PF₆	S10
Figure S1. Photograph of a dye-sensitised TiO ₂ /FTO electrode	S11
Figure S2. Description of ‘ <i>Saubrigues</i> ’ photoelectrochemical cells	S11
Figure S3. UV-vis spectra of dyes in solution	S12
Table S2. Dye concentration on TiO ₂ /FTO	S12
Figure S4. ATR-FTIR of dye-sensitised TiO ₂ /FTO electrode versus powder	S13
Table S3. Peak absorbances and ICP-MS data for RuAc/FTO/TiO₂ , RuP/FTO/TiO₂ and RuNPhAcAc/FTO/TiO₂	S14
Table S4. Peak absorbances and ICP-MS data for RuNPhSiSi/FTO/TiO₂ and RuNPhAcSi/FTO/TiO₂	S15
Figure S5. Comparison of the UV-vis and ICP-MS data	S16
Figure S6. Linear sweep voltammetry	S17
Figure S7. UV-vis spectra of photoelectrodes before and after chronoamperometric oxidation of 1 M Na ₂ SO ₃	S17
Table S5. Juxtaposition of photoelectrooxidation performance of photoanodes in 1 M Na ₂ SO ₃ / 0.1 M Phosphate buffer (pH 7) and in 0.1 M Phosphate buffer (pH 6).	S18
Figure S8. Chronoamperograms for RuNPhSiSi/TiO₂/FTO	S19
Figure S9. Chronoamperograms for RuAc/TiO₂/FTO	S19
Figure S10. Chronoamperograms for RuNPhAcSi/TiO₂/FTO	S19
Table S6. Photoelectrooxidation performance and stability of RuNPhSiSi/FTO/TiO₂	S20
Table S7. Photocurrent densities normalised to the electrode surface area for RuAc/FTO/TiO₂ , RuP/FTO/TiO₂ and RuNPhAcAc/FTO/TiO₂	S21

Table S8. Photocurrent densities normalised to the electrode surface area for RuNPhSiSi/FTO/TiO₂ and RuNPhAcSi/FTO/TiO₂ .	S22
Figure S11. UV-vis spectra of RuAc/TiO₂/FTO before and after experiments in 0.5 M NaClO ₄	S23
Figure S12. UV-vis spectra of RuAc/TiO₂/FTO before and after experiments in 0.1 M acetate buffer	S23
Figure S13. UV-vis spectra of RuAc/TiO₂/FTO before and after experiments in 0.1 M phosphate buffer	S23
Figure S14. UV-vis spectra of RuNPhSiSi /TiO₂/FTO before and after experiments in 0.5 M NaClO ₄	S24
Figure S15. UV-vis spectra of RuNPhSiSi /TiO₂/FTO before and after experiments in 0.1 M acetate buffer	S24
Figure S16. UV-vis spectra of RuNPhSiSi /TiO₂/FTO before and after experiments in 0.1 M phosphate buffer	S24
Figure S17. UV-vis spectra of RuNPhAcSi /TiO₂/FTO before and after experiments in 0.5 M NaClO ₄	S25
Figure S18. UV-vis spectra of RuNPhAcSi /TiO₂/FTO before and after experiments in 0.1 M acetate buffer	S25
Figure S19. UV-vis spectra of RuNPhAcSi /TiO₂/FTO before and after experiments in 0.1 M phosphate buffer	S25
Supplementary References	S26

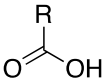
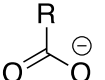
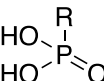
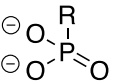
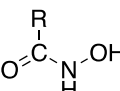
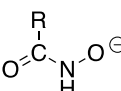
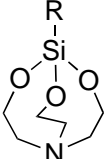
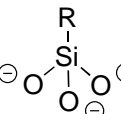
NOMENCLATURE DISCUSSION

As explained in the preface of Nomenclature of Inorganic Chemistry: IUPAC Recommendations 2005, ‘nomenclature must be created to describe new compounds or classes of compounds; modified to resolve ambiguities which might arise; or clarified where there is confusion over the way in which nomenclature should be used. There is also a need to make nomenclature as systematic and uncomplicated as possible in order to assist less familiar users (for example, because they are only in the process of studying chemistry or are non-chemists who need to deal with chemicals at work or at home)’.^{S1}

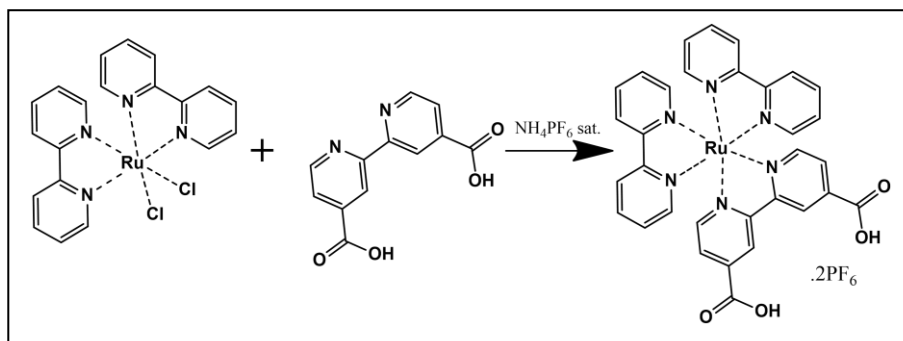
It is common within DS-PEC and DSSC research to specify an anchoring group with a Si-O-M linkage as ‘siloxane’. However, nomenclature set out by IUPAC recommendations states: ‘*Siloxane - Saturated silicon-oxygen hydrides with unbranched or branched chains of **alternating** silicon and oxygen atoms (each silicon atom is separated from its nearest **silicon neighbors** by single oxygen atoms). The general structure of unbranched siloxanes is $H_3Si[OSiH_2]_nOSi_3$* ’.^{S2}

Common anchoring groups in ‘dye-sensitised’ research fields are frequently referred to by either their protonated/protected or deprotonated/deprotected forms (Table S1), as can be witnessed in several DS-PEC reviews serving as exemplars.^{S3-S7} As a result, we feel it is best to both follow this convention in combination with a separate set of IUPAC recommendations. ‘Names of anions derived by formal loss of one or more hydrons from hydroxy groups and their chalcogen analogues (characterised by suffixes such as ‘ol’ and ‘thiol’) are formed by adding the ending ‘ate’ to the appropriate name. Examples: SiH_3O^- - Silanolate’^{S1} Additionally, in this article, we have further specified *Silanetriolate* in order to clarify that there are a total of three Si-O⁻ bonds.

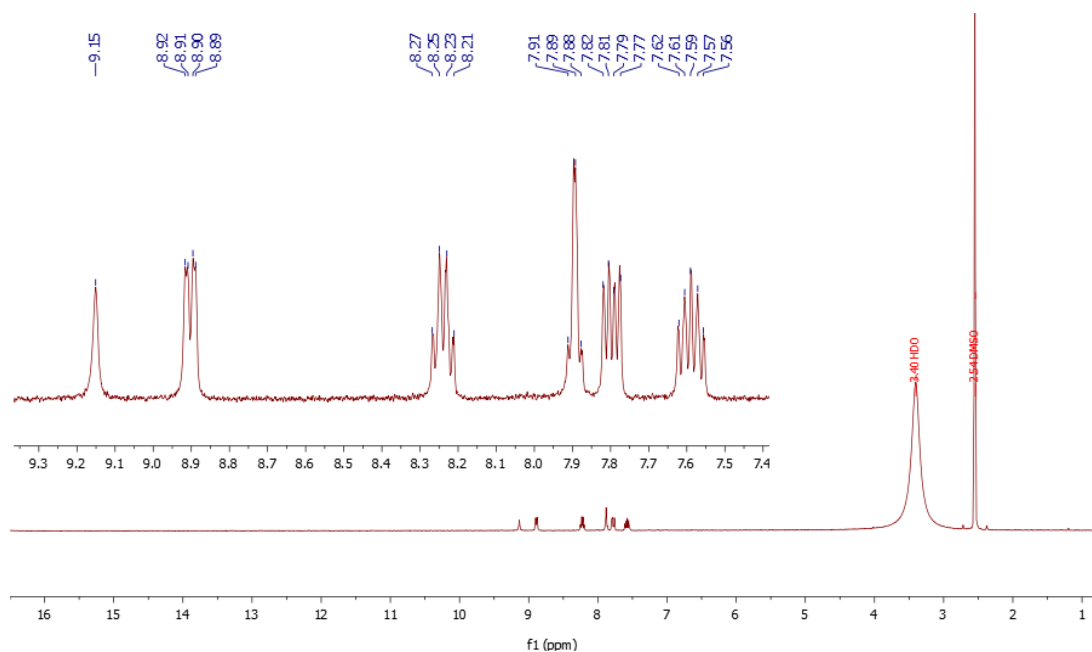
Table S1. Chemical structures and nomenclature for anchoring moieties used in DS-PEC and DSSC research.

Protonated/Protected Structure	Protonated Nomenclature	Deprotonated/Deprotected Structure	Deprotonated Nomenclature
	Carboxylic Acid		Carboxylate
	Phosphonic Acid		Phosphonate
	Hydroxymic Acid		Hydroxymate
	Silatrane		<i>Silanetriolate</i>

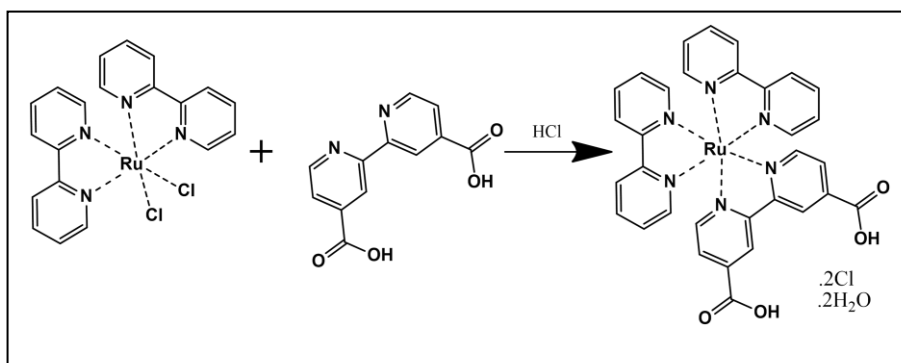
Scheme S1. Synthesis of **RuAc.2PF₆**



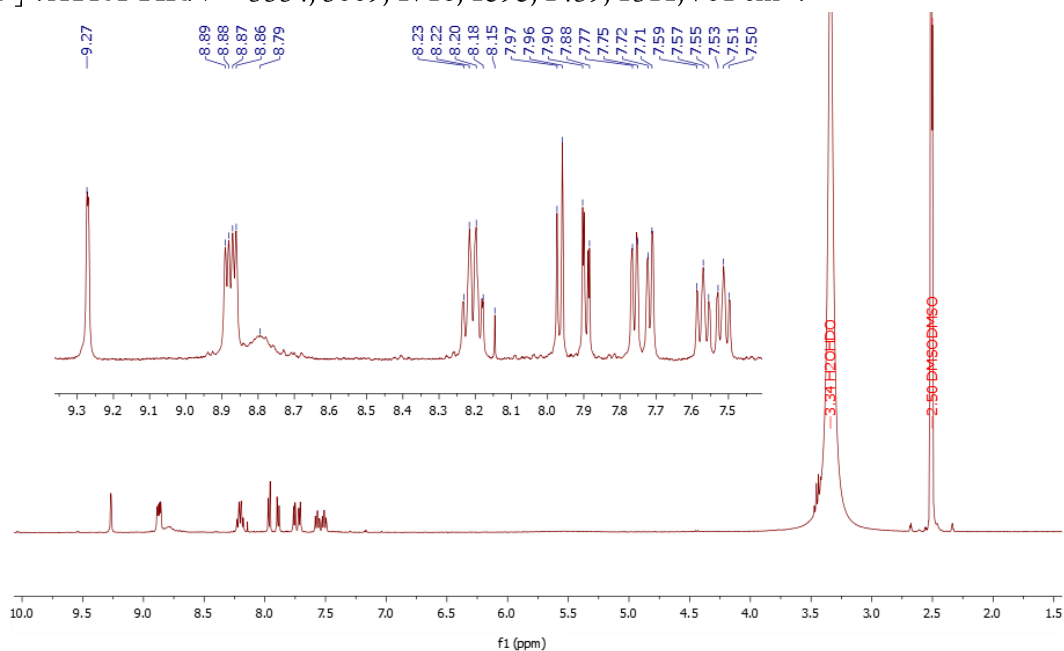
(4,4'-Dicarboxy-2,2'-bipyridine)bis(2,2'-bipyridine)ruthenium-(II) dihexafluorophosphate (**RuAc.2PF₆**):^{S8} *cis*-bis(2,2'-bipyridine)-ruthenium(II) dichloride dihydrate (1 g, 2.06 mmol), 2,2'-bipyridine-4,4'-dicarboxylic acid (605 mg, 2.47 mmol) and NaHCO₃ (1.39 g, 16.5 mmol) were refluxed in a 1:4 water:methanol solution for 8 h. The solution was cooled in an ice-bath and pH was adjusted to 4 using aqueous H₂SO₄ (2 M). The precipitate was filtered and a saturated NH₄PF₆ solution (5 mL) was added to the filtrate. The mixture was then cooled in an ice-bath for 2 h. Excess NH₄PF₆ was removed by filtration, the filtrate was evaporated and the product was then purified with a Sephadex LH-20 column (methanol). The first red fraction was collected to give 833 mg of a black/red microcrystalline pure product. Yield = 43%. ¹H NMR (400 MHz, DMSO-*d*₆): δ = 9.14 (s, 2H), 8.89 (dd, *J* = 8.2, 3.0 Hz, 4H), 8.22 (tdd, *J* = 7.6, 5.6, 1.4 Hz, 4H), 7.92 – 7.83 (m, 4H), 7.78 (ddd, *J* = 11.4, 5.8, 1.4 Hz, 4H), 7.63 – 7.51 (m, 2H). HR-MS (ESI): *m/z* calcd for [RuAc]²⁺ = 658.0903; found: 656,0804 [M-H⁺]⁺.



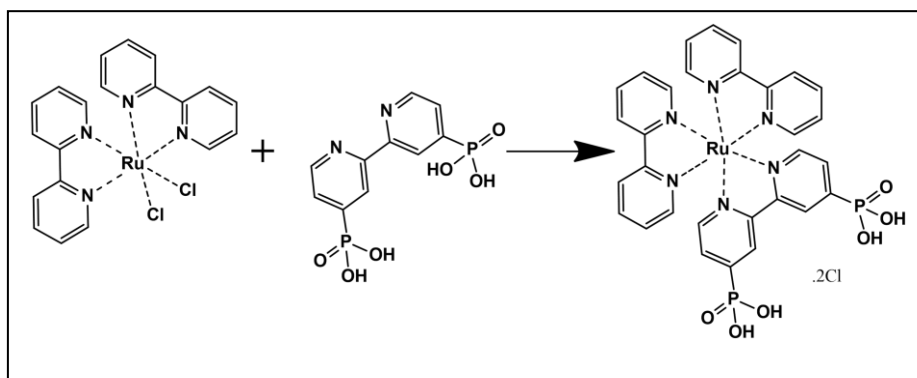
Scheme S2. Synthesis of **RuAc.2Cl.2H₂O**



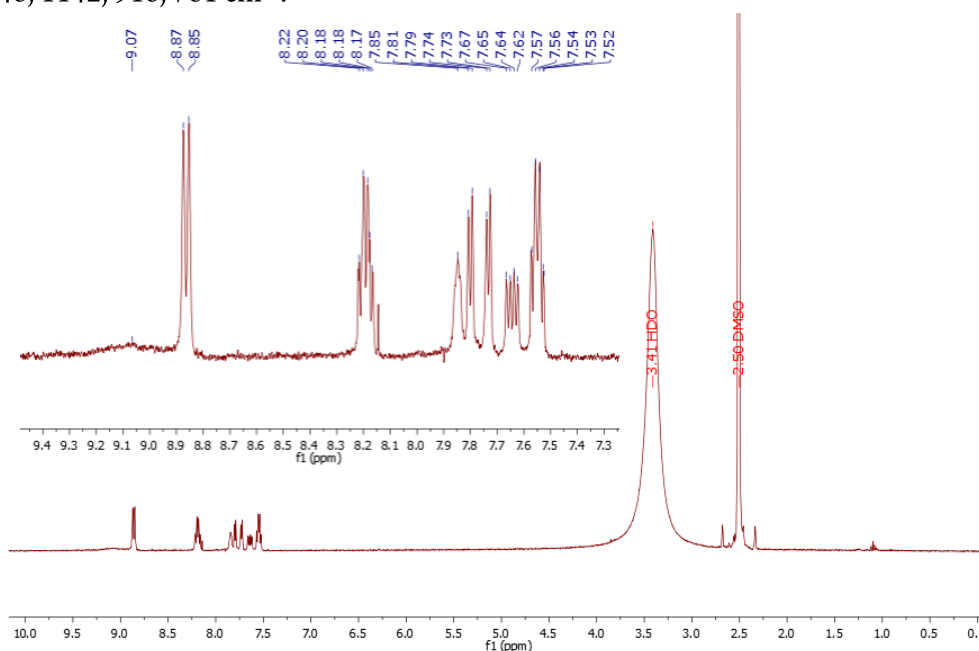
(4,4'-Dicarboxy-2,2'-bipyridine)bis(2,2'-bipyridine)ruthenium-(II) dichloride dihydrate (**RuAc.2Cl.2H₂O**):^{S9} a mixture of 2,2'-bipyridine-4,4'-dicarboxylic acid (500 mg, 1 mmol) and *cis*-bis(2,2'-bipyridine)-ruthenium(II) dichloride dihydrate (302 mg, 1.2 mmol) in 80% acetic acid (20 mL) was stirred for 5 h under reflux, and the solvent was removed *in vacuo*. The resulting dark red solid was dissolved in a minimum amount of ethanol (10 mL) in the presence of 32% concentrated hydrochloric acid (0.2 mL, 10 M). The solution was filtered through Celite, the filtrate was then concentrated to 10 mL, and diacid was precipitated by gradual addition of diethyl ether (50 mL). After stirring for 1 h at room temperature, the dark red product was separated through Büchner filtration, washed with diethyl ether and dried *in vacuo*. Yield = 223 mg (32%); ¹H NMR (400 MHz, DMSO-*d*₆): δ = 9.27 (d, *J* = 1.8 Hz, 2H), 8.88 (dd, *J* = 8.3, 4.0 Hz, 4H), 8.28 – 8.12 (m, 4H), 7.97 (d, *J* = 5.9 Hz, 2H), 7.89 (dd, *J* = 5.9, 1.2 Hz, 2H), 7.74 (ddd, *J* = 18, 5.6, 1.2 Hz, 4H), 7.54 (dddd, *J* = 18, 7.2, 5.6, 1.2 Hz, 4H). HR-MS (ESI): *m/z* calcd for [RuAc]²⁺ = 658.0903; found: 655.0743 [M-H]⁺. ATR-FTIR: ν = 3334, 3069, 1718, 1595, 1439, 1311, 761 cm⁻¹.



Scheme S3. Synthesis of RuP.2Cl

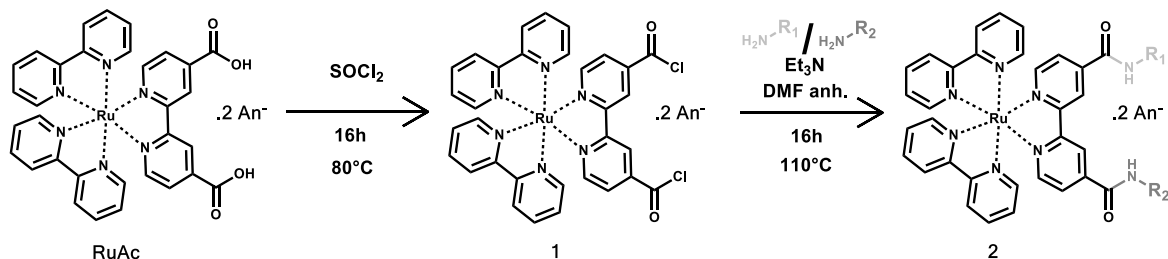


(4,4'-Diphosphonic acid-2,2'-bipyridine)bis(2,2'-bipyridine)ruthenium(II) dichloride dihydrate (**RuP.2Cl**): a mixture of 2,2'-bipyridine-4,4'-diphosphonic acid (200 mg, 0.63 mmol) and *cis*-bis(2,2'-bipyridine)-ruthenium(II) dichloride dihydrate (255 mg, 0.53 mmol) in water (100 mL) was stirred for 5 h under reflux, and the solvent was removed *in vacuo*. The resulting dark red solid was dissolved in a minimum amount of ethanol (5 mL) in the presence of concentrated hydrochloric acid (0.1 mL); the solution was filtered through Celite, the filtrate was then concentrated to 10 mL, and diacid was precipitated by gradual addition of diethyl ether (50 mL). After stirring for 1 h at room temperature, the dark red product was separated through Büchner filtration, washed with diethyl ether and dried *in vacuo*. Yield = 180 mg (42%); ^1H NMR (400 MHz, DMSO- d_6): δ = 8.86 (d, J = 8.3 Hz, 4H), 8.24 – 8.14 (m, 4H), 7.85 (s, 2H), 7.80 (d, J = 5.7 Hz, 2H), 7.73 (d, J = 5.0 Hz, 2H), 7.64 (dd, J = 11.4, 5.5 Hz, 2H), 7.60 – 7.50 (m, 4H). ESI-MS: m/z = 659.01 $[\text{M}+\text{H}]^+$. HR-MS (ESI): m/z calcd for $[\text{RuP}]^{2+}$ = 730.0433; found: 727.022 $[\text{M}-\text{H}]^+$. ATR-FTIR: ν = 3353, 3076, 1601, 1446, 1142, 916, 761 cm^{-1} .



PEPTIDE COUPLING SYNTHESIS METHODOLOGY

RuNPhSiLSiL.2PF₆, **RuNPhAcSi.2Cl** and **RuNPhAcAc.2PF₆** were obtained following the peptide coupling reaction (4,4'-Dicarboxy-2,2'-bipyridine)bis(2,2'-bipyridine)ruthenium(II) (**RuAc**) and the aminophenyl derivatives presenting the chosen anchor (H₂N-R1, H₂N-R2 or both).

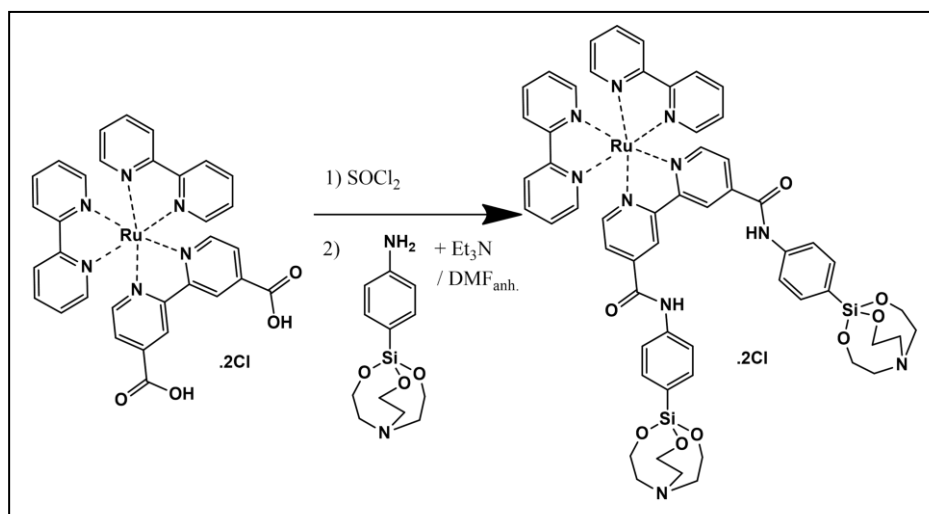


The acyl chloride intermediate **1** was prepared by refluxing a solution of **RuAc** dissolved in few milliliters of SOCl₂ under dry N₂ atmosphere for 16 hours in the dark. After completion of the first step, SOCl₂ was evaporated by flowing dry N₂ for 2 hours at room temperature. A sticky black red solid should become visible at the bottom of the reaction flask before proceeding to the second step.

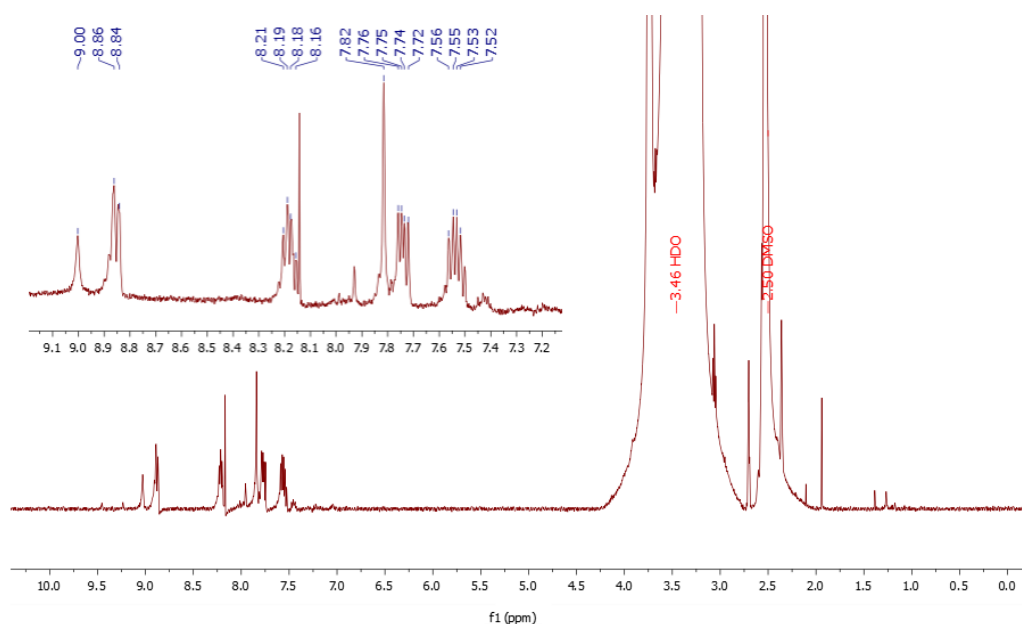
Further, a solution of 2 equivalents of a chosen aminophenyl completely solubilised in anhydrous DMF was prepared inside a nitrogen-filled glovebox and was then added to solid **1** under stirring in N₂ atmosphere. A solution of 2 equivalents of triethylamine in anhydrous DMF was then injected to trigger the reaction. A corrosive white fume should be seen inside the flask. The reaction was then left at 110°C for 16 hours. DMF was removed *in vacuo* giving a dark red wax at the bottom of the flask.

Attempts to purify **2** via filtration and chromatography (Silica, Alumina, LH-20 or C25 Sephadex) were unsuccessful due to their poor solubility in common solvents, size and strong affinity to metal oxides. Therefore, purification was performed via extraction with acetonitrile using a homemade Soxhlet apparatus for 16 hours. The extraction was considered complete when the starting suspension was essentially colourless and a red pure solid **2** was formed at the bottom of the extractor chamber. The solid was collected, dried under vacuum and kept in the dark to prevent any photodegradation. Unreacted **RuAc** present in the Soxhlet filtrate solution can be recycled using a LH-20 Sephadex column (water).

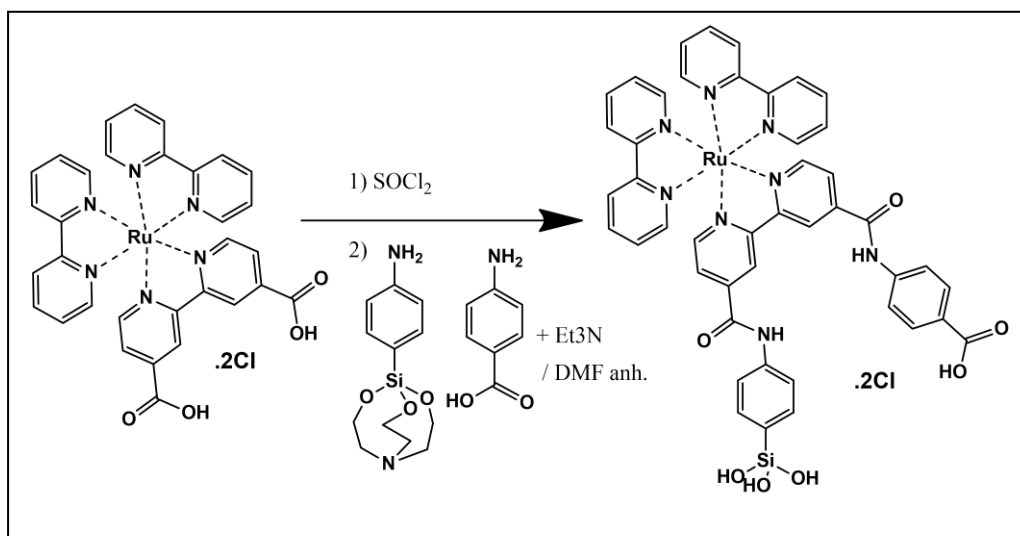
Scheme S4. Synthesis of **RuNPhSiSiL.2PF₆**



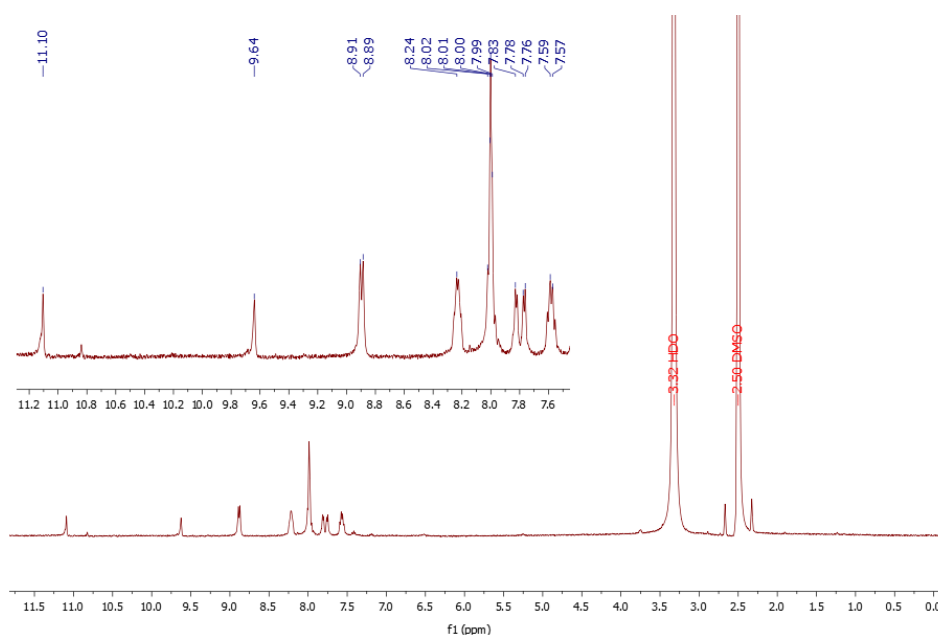
4,4'-(Diphenyldisilatrane)-dicarboxamide-2,2'-bipyridine)bis(2,2'-bipyridine)ruthenium-(II) dihexafluorophosphate (**RuNPhSiSiL.2PF₆**): the complex was prepared following peptide coupling method (see page S7) starting with (4,4'-dicarboxy-2,2'-bipyridine)bis(2,2'-bipyridine)ruthenium-(II) dihexafluorophosphate (100 mg, 0.105 mmol) and SOCl₂ (5 mL, 69 mmol). After formation of the acyl chloride intermediate, p-aminobenzylsilatrane solution (59 mg, 0.22 mmol in 5 mL of anhydrous DMF) and then triethylamine solution (29 μ L, 0.21 mmol in 5 mL anhydrous DMF) were added. After 16 hours of Soxhlet extraction with acetonitrile, 40 mg of red solid were collected and dried under vacuum. Yield = 26%. ¹H NMR (400 MHz, D₂O-*d*₆): δ = 9.00 (s, 2H), 8.85 (d, *J* = 8.4 Hz, 4H), 8.27 – 8.15 (m, 4H), 7.82 (s, 4H), 7.74 (dd, *J* = 10.1, 5.7 Hz, 4H), 7.61 – 7.49 (m, 6H), HR-MS (ESI): *m/z* calcd for [RuNPhSiSiL]²⁺ = 1154.2865; found: 1153.5061 [M-H]⁺. ATR-FTIR: ν = 3302, 3153, 1608, 1394, 1084, 1007, 910 cm⁻¹.



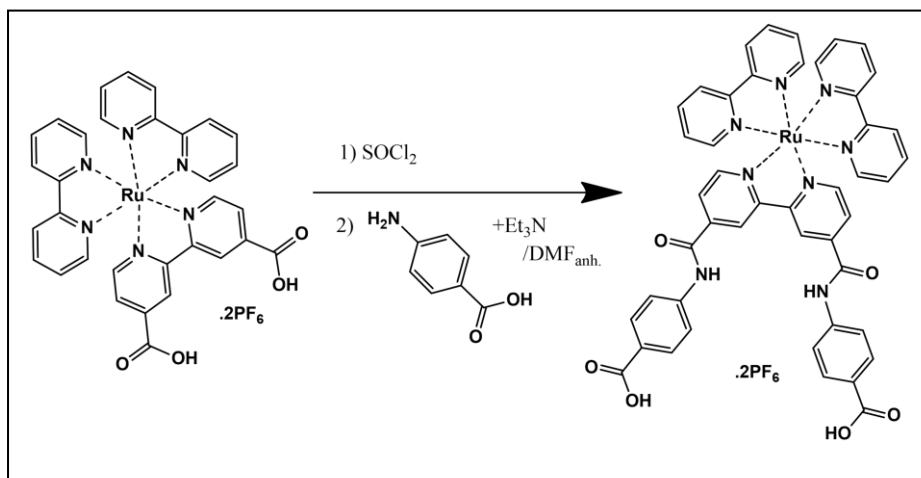
Scheme S5. Synthesis of RuNPhAcSi.2Cl



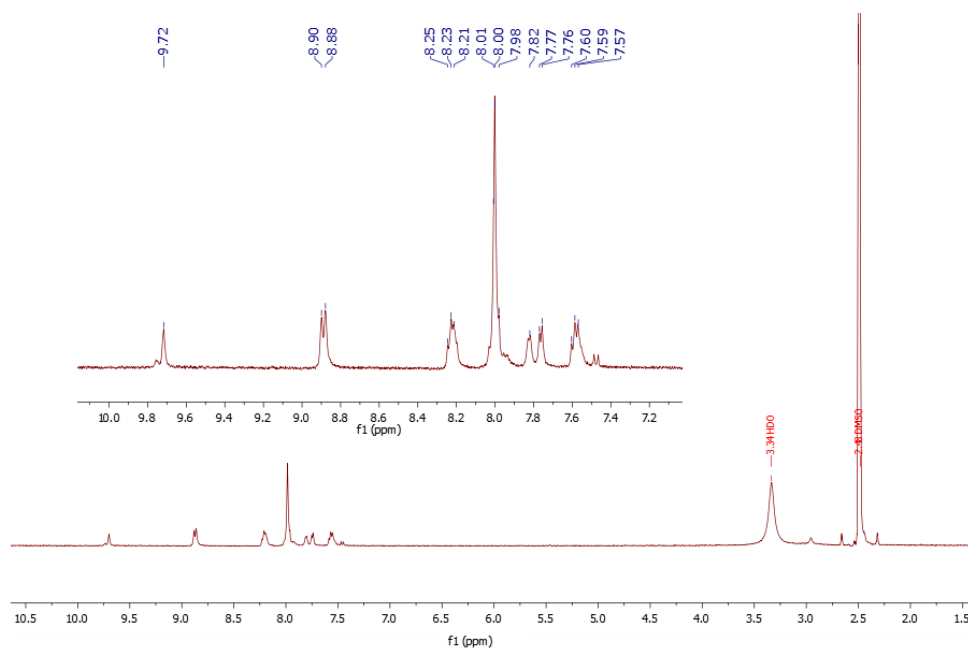
(4,4'-(Phenylsilanetriol)-(phenylcarboxylic acid)-dicarboxamide-2,2'-bipyridine)bis(2,2'-bipyridine)ruthenium(II) dichloride (**RuNPhAcSi.2Cl**): the complex was prepared following peptide coupling method (see page S7) starting with (4,4'-dicarboxy-2,2'-bipyridine)bis(2,2'-bipyridine)ruthenium(II) dichloride dihydrate (100 mg, 0.105 mmol) and SOCl_2 (5 mL, 69 mmol). After formation of the acyl chloride intermediate, p-aminobenzylsilatrane (28 mg, 0.105 mmol) and 4-aminobenzoic acid (14 mg, 0.105 mmol) dissolved in 5 ml anhydrous DMF and then triethylamine solution (29 μL , 0.21 mmol in 5 ml anhydrous DMF) were added. After 16 hours of Soxhlet extraction with acetonitrile, 31.5 mg of red solid were collected and dried under vacuum. Yield = 30 %. ^1H NMR (400 MHz, $\text{DMSO}-d_6$): δ = 11.10 (s, 2H), 9.64 (s, 2H), 8.90 (d, J = 8.3 Hz, 6H), 8.24 (s, 6H), 8.05 – 7.96 (m, 6H), 7.83 (s, 4H), 7.77 (d, J = 5.8 Hz, 4H). HR-MS (ESI): m/z calcd for $[\text{RuNPhAcSi}]^{2+}$ = 730.1520; found: 929.1216 $[\text{M}-\text{H}^+]^+$. ATR-FTIR: ν = 3341, 3237, 3044, 1679, 1595, 1524, 1407, 1317, 1232, 1104, 864, 761 cm^{-1} .



Scheme S6. Synthesis of **RuNPhAcAc.2PF₆**



(4,4'-(Diphenyldicarboxylic acid)-dicarboxamide)-bis(2,2'-bipyridine)ruthenium-(II) dihexafluorophosphate (**RuNPhAcAc.2PF₆**): the complex was prepared following peptide coupling method (see page S7) starting with (4,4'-Dicarboxy-2,2'-bipyridine)bis(2,2'-bipyridine)ruthenium-(II) dichloride dihydrate (150 mg, 0.158 mmol) and SOCl₂ (5 mL, 69 mmol). After formation of the acyl chloride intermediate, 4-aminobenzoic acid solution (46 mg, 0.332 mmol in 5 ml anhydrous DMF) and then of triethylamine solution (44 μ L, 0.32 mmol in 5 mL anhydrous DMF) were added. After 16 hours of Soxhlet extraction with acetonitrile, 103 mg of red solid was still present inside the extraction chamber was collected and dried under vacuum Yield = 60%. ¹H NMR (400 MHz, DMSO-*d*₆): δ = 9.72 (s, 2H), 8.89 (d, *J* = 8.3 Hz, 4H), 8.27 – 8.13 (m, 6H), 8.00 (d, *J* = 2.9 Hz, 12H), 7.84 – 7.73 (m, 4H), 7.63 – 7.54 (m, 4H). HR-MS (ESI): *m/z* calcd for [RuNPhAcAc]²⁺ = 896.1645, found: 895.1576 [M+H]⁺. ATR-FTIR: ν = 3379, 3231, 3056, 1672, 1595, 1530, 1414, 1310, 1239, 1181, 1051, 754 cm⁻¹.



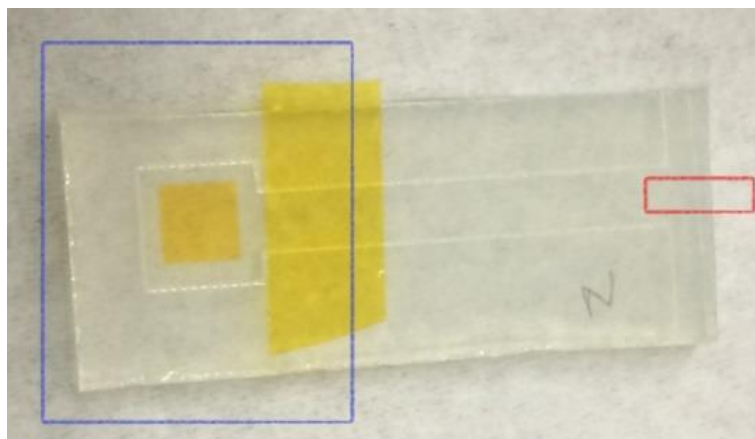


Figure S1. Photograph of a dye-sensitised TiO_2/FTO electrode used for photoelectrochemical measurements. Electrical connection to the electrodes was at the FTO surface outside the cell (*red rectangle*). An insulating polyimide tape (Kapton) was applied to keep only the square area of the laser-engraved FTO area exposed to the electrolyte solution (*blue rectangle*).

PHOTOELECTROCHEMICAL 'SAUBRIGUES' CELL

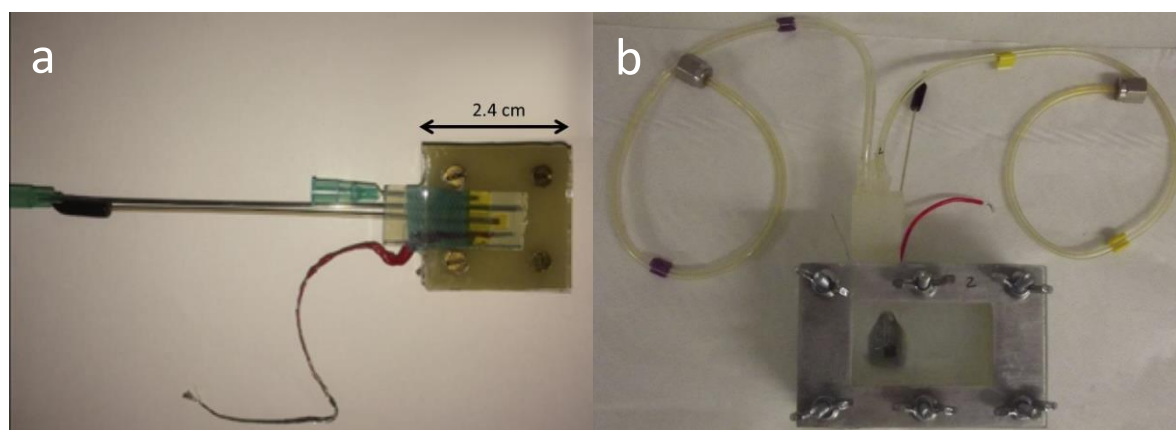


Figure S2. Photographs of (a) small and (b) large 'Saubrigues' cells.

Two custom-made photoelectrochemical 'Saubrigues' cells were specifically built for this study. Each cell was composed of two thick slides of glass separated by an elastic polymer with a photoelectrochemical chamber in the centre. Nuts and bolts at the corners of the cell were used to compress the glass and polymer layers, preventing any leaks of gas or liquid. A small model (Figure S2a) was used for photoelectrochemical experiments involving 'stress' conditions. The larger model (Figure S2b) was used for photoelectrochemical measurements in the presence of sodium sulphite.

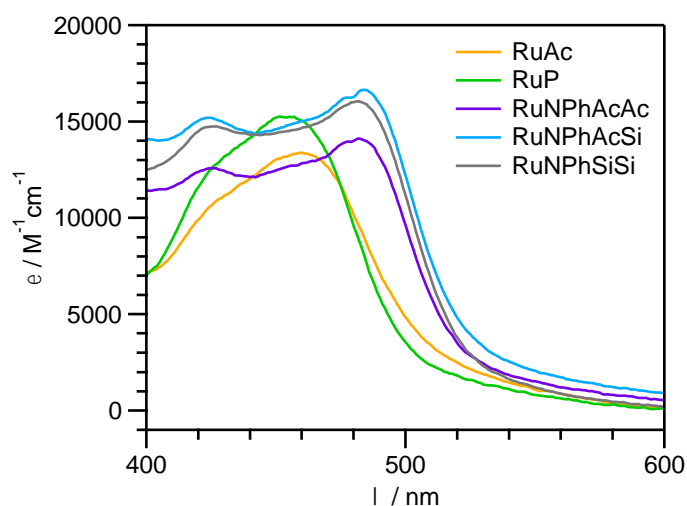


Figure S3. UV-vis absorption spectra of **RuAc** (*orange*), **RuP** (*green*), **RuNPhAcAc** (*purple*), **RuNPhAcSi** (*cyan*), **RuNPhSiSi** (*grey*) in 0.1 M acetate buffer.

Table S2. The amounts of dyes adsorbed on TiO₂/FTO (nmol cm⁻²_{geom.}).^a

Sensitiser	Lowest	Highest	Average ± one standard deviation
RuAc	33	114	60 ± 20
RuNPhSiSi	7	37	19 ± 11
RuNPhAcSi	22	47	32 ± 6
RuNPhAcAc	47	105	75 ± 19
RuP	43	55	49 ± 5

^a Determined by ICP-MS for similarly prepared 45 **RuNPhSiSi**/TiO₂/FTO, 45 **RuNPhAcSi**/TiO₂/FTO, 42 **RuAc**/TiO₂/FTO, 12 **RuP**/TiO₂/FTO, and 6 **RuNPhAcAc**/TiO₂/FTO electrodes.

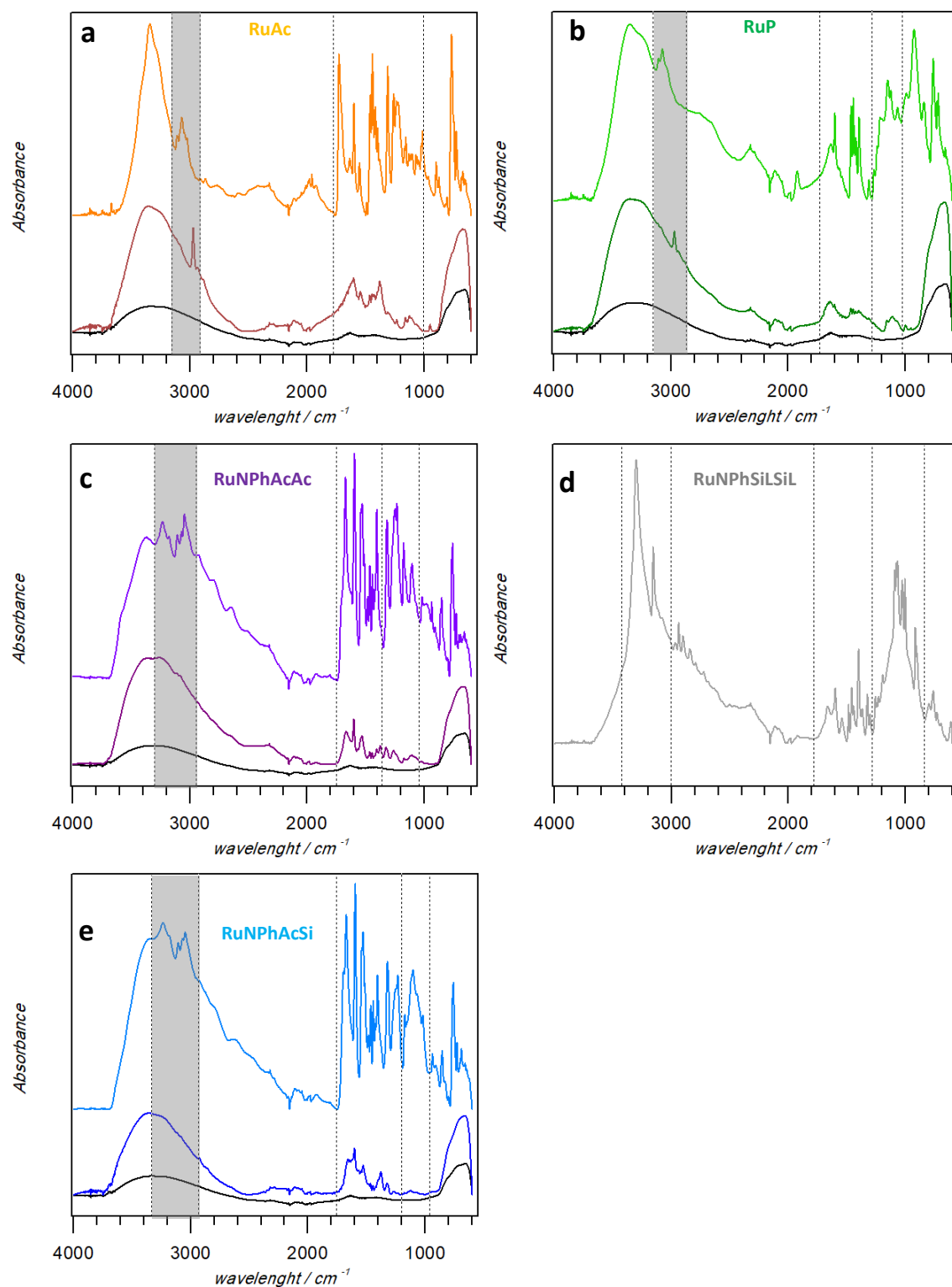


Figure S4. ATR-FTIR spectra of (a) **RuAc**, (b) **RuP**, (c) **RuNPhAcAc**, (d) **RuNPhSiLSiL** and (e) **RuNPhAcSi** analysed as a freestanding powder (light colour, upper curves) and when adsorbed onto a mesoporous TiO_2 film (dark colour, bottom curves). Black curves show spectra of unmodified mesoporous TiO_2 support. Peaks in the shaded areas are characteristic for $-\text{OH}$ hydroxide bands.

Table S3. Peak absorbances and ICP-MS data for **RuAc**/FTO/TiO₂, **RuP**/FTO/TiO₂ and **RuNPhAcAc**/FTO/TiO₂ anodes pre-and post-chronoamperometric measurements.

Dye	Electrolyte	pH	Dye loading / nmol cm ^{-2a}	Peak Absorbance		ICP-MS / nmol cm ⁻²	
				Initial ^b	Final ^b	Electrode ^c	Solution ^c
RuAc	NaClO ₄ (0.5 M)	1	99	0.47	0.08	5.0	94
		2	114	0.50	0.07	15	99
		3	91	0.62	0.18	17	74
		4	104	0.61	0.08	5.2	99
		5	70	0.51	0.04	4.2	66
		6	55	0.60	0.05	3.3	52
		7	80	0.59	0.06	4.0	76
		8	77	0.67	0.10	5.4	72
	Acetate buffer (0.1 M)	4	44	0.52	0.10	8.4	36
		5	70	0.60	0.09	6.3	64
		5.6	56	0.44	0.02	4.5	52
	Phosphate buffer (0.1 M)	6	39	0.47	0.05	11	28
		7	47	0.52	0.05	6.1	41
		8	33	0.41	0.05	3.0	30
	Na ₂ SO ₃ (1 M) Phosphate buffer (0.1 M)	7	98	0.51	0.05	0.98	97
RuP	NaClO ₄ (0.5 M)	6	99	0.80	0.17	5.0	94
	Phosphate buffer (0.1 M)	6	114	0.68	0.10	15	99
	Na ₂ SO ₃ (1 M) Phosphate buffer (0.1 M)	7	46	0.54	0.05	2.8	43
RuNPhAcAc	Na ₂ SO ₃ (1 M) Phosphate buffer (0.1 M)	7	101	0.69	0.04	4.0	97

^a Determined by ICP-MS. ^b Absorbance peaks measured before or after photoelectrochemical test; λ_{max} = RuAc - 458 nm; RuP - 447 nm; RuNPhAcAc - 489 nm. ^c Amount of ruthenium present on the surface and in solution after photoelectrochemical tests.

Table S4. Peak absorbances and ICP-MS data for **RuNPhSiSi/FTO/TiO₂**, and **RuNPhAcSi/FTO/TiO₂** anodes pre-and post-chronoamperometric measurements.

Dye	Electrolyte	pH	Dye loading / nmol cm ^{-2a}	Peak Absorbance		ICP-MS / nmol cm ⁻²	
				Initial ^b	Final ^b	Electrode ^c	Solution ^c
RuNPhSiSi	NaClO ₄ (0.5 M)	1	10	0.16	0.11	9.3	0.7
		2	36	0.18	0.11	34	1.8
		3	21	0.17	0.16	21	0.21
		4	17	0.17	0.23	17	0.34
		5	12	0.27	0.26	12	0.36
		6	8	0.16	0.13	7.8	0.16
		7	10	0.23	0.17	9.7	0.3
		8	20	0.19	0.15	20	0.2
		9	15	0.21	0.14	15	0.15
	Acetate buffer (0.1 M)	4	11	0.2	0.17	11	0.11
		5	22	0.19	0.19	21	0.66
		5.6	10	0.18	0.16	9.9	0.1
	Phosphate buffer (0.1 M)	6	11	0.14	0.12	10	0.55
		7	9	0.12	0.06	8.5	0.54
		8	15	0.13	0.07	14	0.6
	Na ₂ SO ₃ (1 M) Phosphate buffer (0.1 M)	7	9	0.14	0.09	8.9	0.09
RuNPhAcSi	NaClO ₄ (0.5 M)	1	31	0.44	0.33	24	6.8
		2	38	0.36	0.30	35	3.4
		3	36	0.48	0.38	33	2.5
		4	31	0.38	0.29	29	2.2
		5	37	0.48	0.32	34	2.6
		6	47	0.4	0.32	44	3.3
		7	38	0.42	0.32	36	2.3
		8	32	0.48	0.35	29	2.6
		9	33	0.49	0.35	29	3.6
	Acetate buffer (0.1 M)	4	41	0.40	0.29	38	2.9
		5	38	0.36	0.31	36	2.3
		5.6	23	0.33	0.32	22	1.2
	Phosphate buffer (0.1 M)	6	31	0.41	0.34	29	2.2
		7	25	0.31	0.22	23	1.8
		8	29	0.39	0.28	27	2.0
	Na ₂ SO ₃ (1 M) Phosphate buffer (0.1 M)	7	20	0.29	0.2	14	6.3

^a Determined by ICP-MS. ^b Absorbance peaks measured before or after photoelectrochemical test; λ_{max} = RuNPhSiSi - 482 nm; RuNPhAcSi - 482 nm. ^c Amount of ruthenium present on the surface and in solution after photoelectrochemical tests.

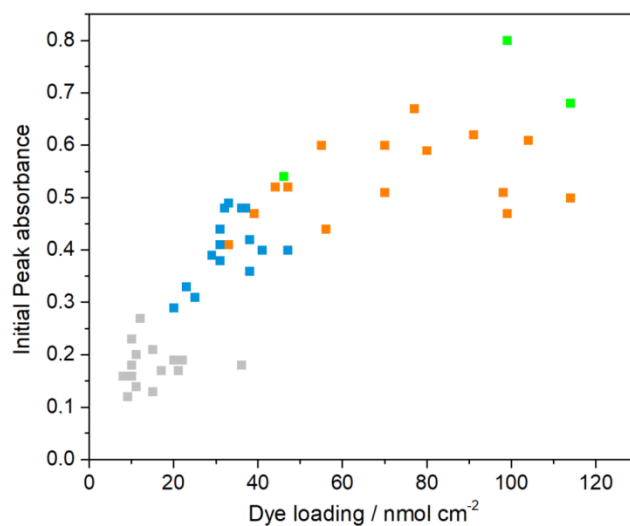


Figure S5. Initial peak absorbance derived from UV-vis spectra vs. the dye loading inferred from ICP-MS analysis for **RuAc**/TiO₂/FTO (*orange*), **RuP**/TiO₂/FTO (*green*), **RuNPhSiSi**/TiO₂/FTO (*grey*) and **RuNPhAcSi**/TiO₂/FTO (*blue*) photoanodes.

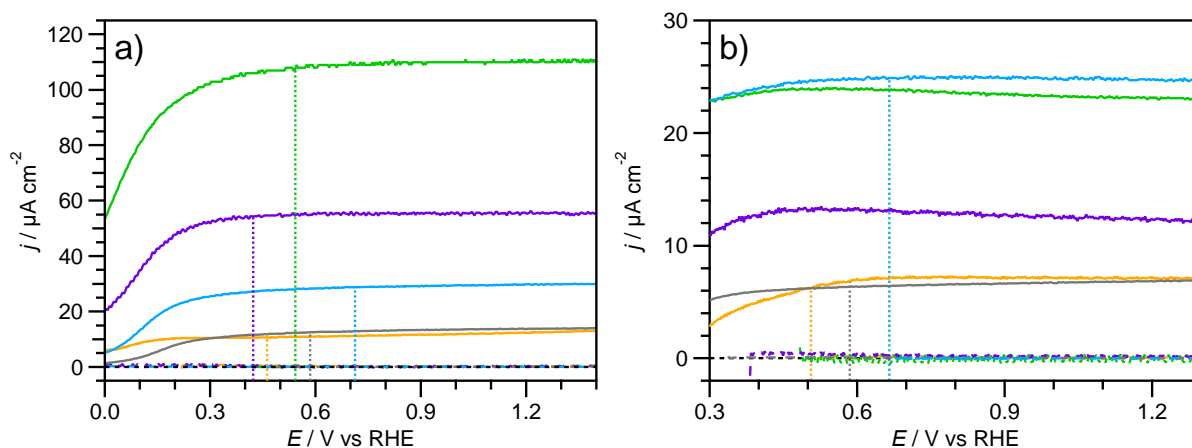


Figure S6. Linear sweep voltammograms (scan rate 0.010 V s^{-1}) for **RuAc**/ TiO_2 /FTO (orange), **RuP**/ TiO_2 /FTO (green), **RuNPhAcAc**/ TiO_2 /FTO (purple); **RuNPhSiSi**/ TiO_2 /FTO (grey), and **RuNPhAcSi**/ TiO_2 /FTO (cyan) in contact with argon-saturated $1.0 \text{ M Na}_2\text{SO}_3$ buffered with (a) phosphate (1.0 M , $\text{pH } 7.0$) and (b) acetate (0.1 M , $\text{pH } 4.0$). Measurements were undertaken in the dark (dashed lines) and under 1 sun visible light irradiation (solid lines). Potentials used to record chronoamperograms shown in Figure 2, Figure 3 and Figures S6-8 are indicated by vertical dotted lines.

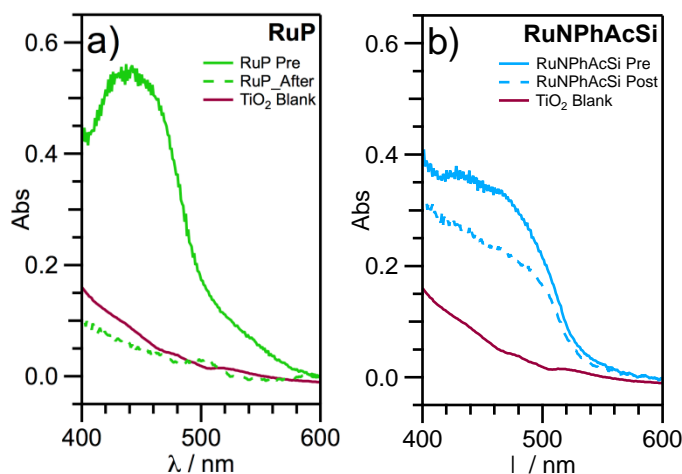


Figure S7. UV-vis absorption spectra of (a) **RuP**/ TiO_2 /FTO (green); and (b) **RuNPhAcSi**/ TiO_2 /FTO (cyan) before (solid lines) and after (dashed lines) photoelectrochemical oxidation of aqueous $1.0 \text{ M Na}_2\text{SO}_3$ in phosphate buffer (1.0 M , $\text{pH } 7.0$) shown in Figure 2 (main text). Dark red curves show background spectra for TiO_2 /FTO.

Table S5. Juxtaposition of photoelectrooxidation performance of the investigated dye-sensitised anodes in 1 M Na₂SO₃ / 0.1 M Phosphate buffer (pH 7) and 0.1 M Phosphate buffer (pH 6).

Electrolyte	Dye	Dye loading / nmol cm ^{-2a}	i_{hv} / A mol ^{-1b}		Ru loss / % (ICP-MS)	Dye loss / % (UV-vis ^c)
			10 min	80 min		
Na ₂ SO ₃ (1 M) Phosphate buffer (0.1 M, pH 7)	RuAc	98	220	97	98	99
	RuP	46	3900	1300	99	94
	RuNPhAcAc	101	140	44	99	96
	RuNPhSiSi	9.0	460	420	5.0	1.0
	RuNPhAcSi	20	4500	3700	30	31
Phosphate buffer (0.1 M, pH 6)	RuAc	39	64	16	71	90
	RuP	114	64	45	87	96
	RuNPhAcAc		not measured			
	RuNPhSiSi	11	120	96	5.0	7.0
	RuNPhAcSi	31	190	170	7.0	17

^a Determined by ICP-MS. ^b Derived from chronoamperograms measured under 1 sun irradiation in quiescent Ar-saturated solutions; currents are normalised to the amount of dye initially adsorbed on the electrode.

^c Calculated as a ratio of absorbance at λ_{max} (RuAc - 458 nm; RuP - 447 nm; RuNPhAcAc - 489 nm; RuNPhSiSi - 482 nm; RuNPhAcSi - 482 nm).

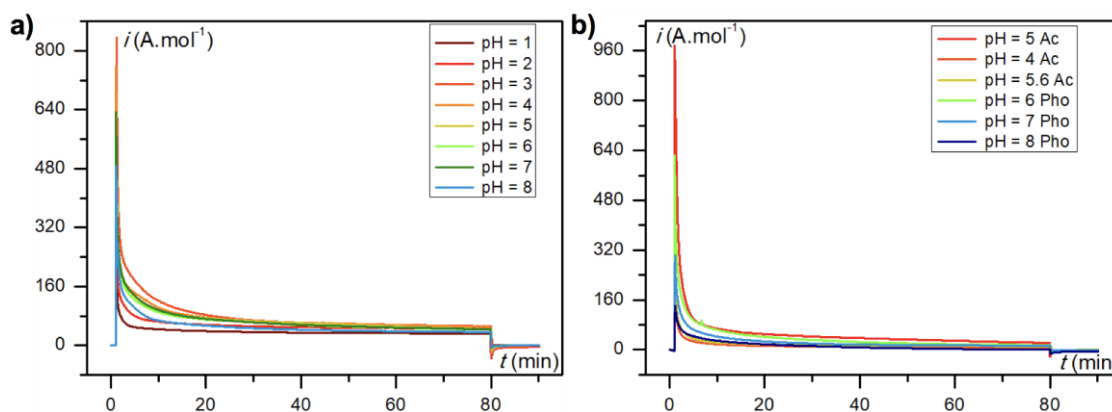


Figure S8. Chronoamperograms for photoelectrooxidation (1 sun, $\lambda > 400$ nm) of aqueous (a) 0.5 M NaClO₄, and (b) 0.1 M phosphate buffer and acetate buffer at different pH by FTO/TiO₂/RuAc. Measurements were undertaken with argon-saturated solutions. Currents are normalised to the amount of dye initially adsorbed on the electrode surface.

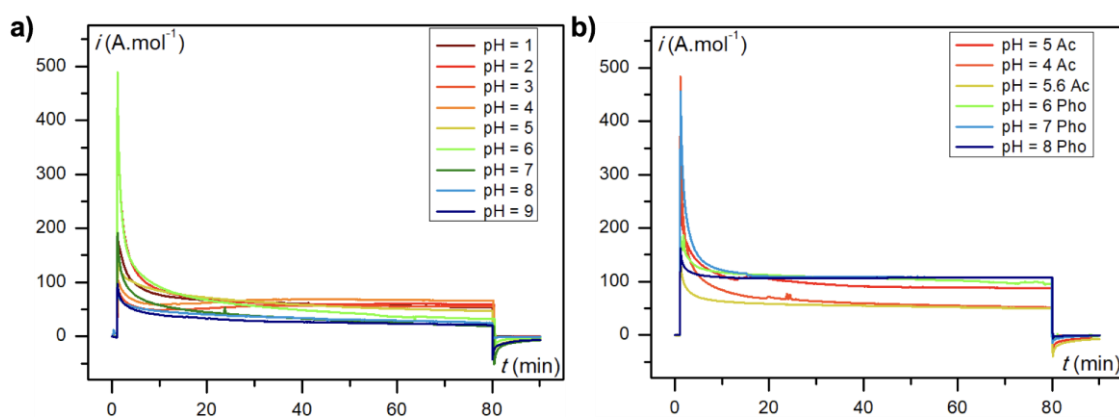


Figure S9. Chronoamperograms for photoelectrooxidation (1 sun, $\lambda > 400$ nm) of aqueous (a) 0.5 M NaClO₄, (b) 0.1 M phosphate buffer and acetate buffer at different pH by FTO/TiO₂/RuNPhSiSi. Measurements were undertaken with argon-saturated solutions. Currents are normalised to the amount of dye initially adsorbed on the electrode surface.

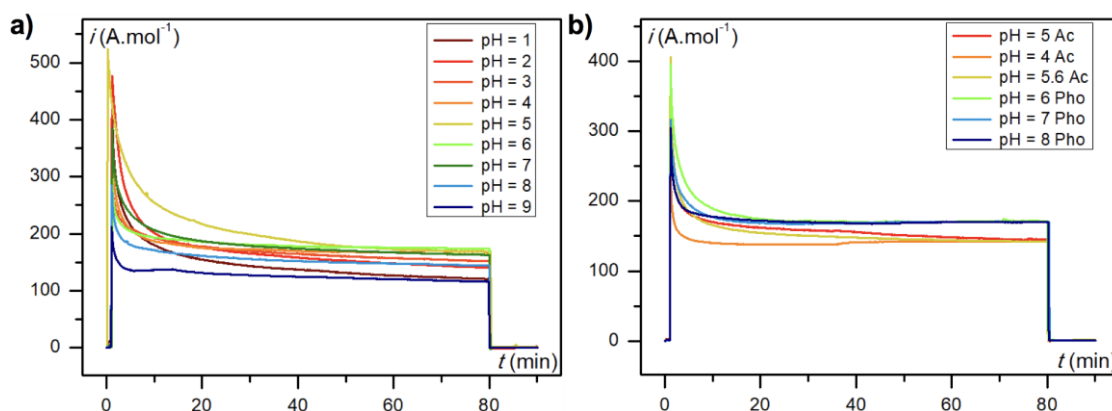


Figure S10. Chronoamperograms for photoelectrooxidation (1 sun, $\lambda > 400$ nm) of aqueous (a) 0.5 M NaClO₄, (c) 0.1 M phosphate buffer and acetate buffer at different pH by FTO/TiO₂/RuNPhAcSi. Measurements were undertaken with argon-saturated solutions. Currents are normalised to the amount of dye initially adsorbed on the electrode surface.

Table S6. Photoelectrooxidation performance and stability of the RuNPhSiSi/FTO/TiO₂ anodes.

Electrolyte	pH	Dye loading / nmol cm ⁻² ^a	i_{hv} / A mol ⁻¹ ^b		Ru loss/ % (ICP-MS)	Dye loss / % (UV-vis) ^c
			10 min	80 min		
NaClO ₄ (0.5 M)	1.0	10	77	53	7	32
	2.0	36	86	60	5	36
	3.0	21	49	55	1	5
	4.0	17	59	66	2	0
	5.0	12	84	47	3	5
	6.0	8.0	92	33	2	20
	7.0	10	58	19	3	30
	8.0	20	47	24	1	30
	9.0	15	40	21	1	22
Acetate buffer (0.1 M)	4.0	11	111	87	1	17
	5.0	22	84	52	3	4
	5.6	10	63	50	1	9
Phosphate buffer (0.1 M)	6.0	11	117	96	5	7
	7.0	9.0	121	107	6	48
	8.0	15	108	107	4	49

^a Determined by ICP-MS. ^b Derived from chronoamperograms measured under 1 sun irradiation in quiescent Ar-saturated solutions; currents are normalised to the amount of dye initially adsorbed on the electrode determined by ICP-MS. ^c Calculated as a ratio of absorbance at $\lambda_{\text{max}} = 482$ nm before and after photoelectrochemical test.

Table S7. Photoelectrooxidation current densities normalised to the electrode surface area for **RuAc**/FTO/TiO₂, **RuP**/FTO/TiO₂ and **RuNPhAcAc**/FTO/TiO₂.

Dye	Electrolyte	pH	Dye loading / nmol cm ⁻² ^a	j_{hv} / $\mu\text{A cm}^{-2}$ ^b	
				10 min	80 min
RuAc	NaClO ₄ (0.5 M)	1	99	4.3	3.2
		2	114	7.3	5.1
		3	91	11	4.7
		4	104	11	5.1
		5	70	6.7	3.0
		6	55	4.9	2.4
		7	80	7.7	3.4
		8	77	5.1	2.8
	Acetate buffer (0.1 M)	4	44	3.0	0.97
		5	70	1.3	0.49
		5.6	56	1.3	0.62
	Phosphate buffer (0.1 M)	6	39	2.5	0.62
		7	47	2.0	0.61
		8	33	0.96	0.00
	Na ₂ SO ₃ (1 M) Phosphate buffer (0.1 M)	7	98	21	9.5
RuP	NaClO ₄ (0.5 M)	6	99	4.3	3.2
	Phosphate buffer (0.1 M)	6	114	7.3	5.1
	Na ₂ SO ₃ (1 M) Phosphate buffer (0.1 M)	7	46	180	59
RuNPhAcAc	Na ₂ SO ₃ (1 M) Phosphate buffer (0.1 M)	7	101	14	4.5

^a Determined by ICP-MS. ^b Derived from chronoamperograms measured under 1 sun irradiation in quiescent Ar-saturated solutions.

Table S8. Photoelectrooxidation current densities normalised to the electrode surface area for RuNPhSiSi/FTO/TiO₂ and RuNPhAcSi/FTO/TiO₂.

Dye	Electrolyte	pH	Dye loading / nmol cm ^{-2a}	j_{hv} / $\mu\text{A cm}^{-2b}$	
				10 min	80 min
RuNPhSiSi	NaClO ₄ (0.5 M)	1	10	0.77	0.53
		2	36	3.1	2.2
		3	21	1.0	1.2
		4	17	1.0	1.1
		5	12	1.0	0.56
		6	8	0.74	0.26
		7	10	0.58	0.19
		8	20	0.94	0.48
		9	15	0.60	0.31
	Acetate buffer (0.1 M)	4	11	1.2	0.96
		5	22	1.9	1.1
		5.6	10	0.63	0.50
	Phosphate buffer (0.1 M)	6	11	1.3	1.1
		7	9	1.1	0.96
		8	15	1.6	1.6
	Na ₂ SO ₃ (1 M) Phosphate buffer (0.1 M)	7	9	4.1	3.7
RuNPhAcSi	NaClO ₄ (0.5 M)	1	31	5.6	3.8
		2	38	7.6	5.4
		3	36	7.0	5.5
		4	31	5.8	5.2
		5	37	9.4	6.3
		6	47	9.1	8.2
		7	38	7.9	6.2
		8	32	5.5	4.6
		9	33	4.5	3.8
	Acetate buffer (0.1 M)	4	41	7.0	5.9
		5	38	5.3	5.4
		5.6	23	3.8	3.3
	Phosphate buffer (0.1 M)	6	31	5.9	5.3
		7	25	4.5	4.3
		8	29	5.1	4.9
	Na ₂ SO ₃ (1 M) Phosphate buffer (0.1 M)	7	20	91	74

^a Determined by ICP-MS. ^b Derived from chronoamperograms measured under 1 sun irradiation in quiescent Ar-saturated solutions.

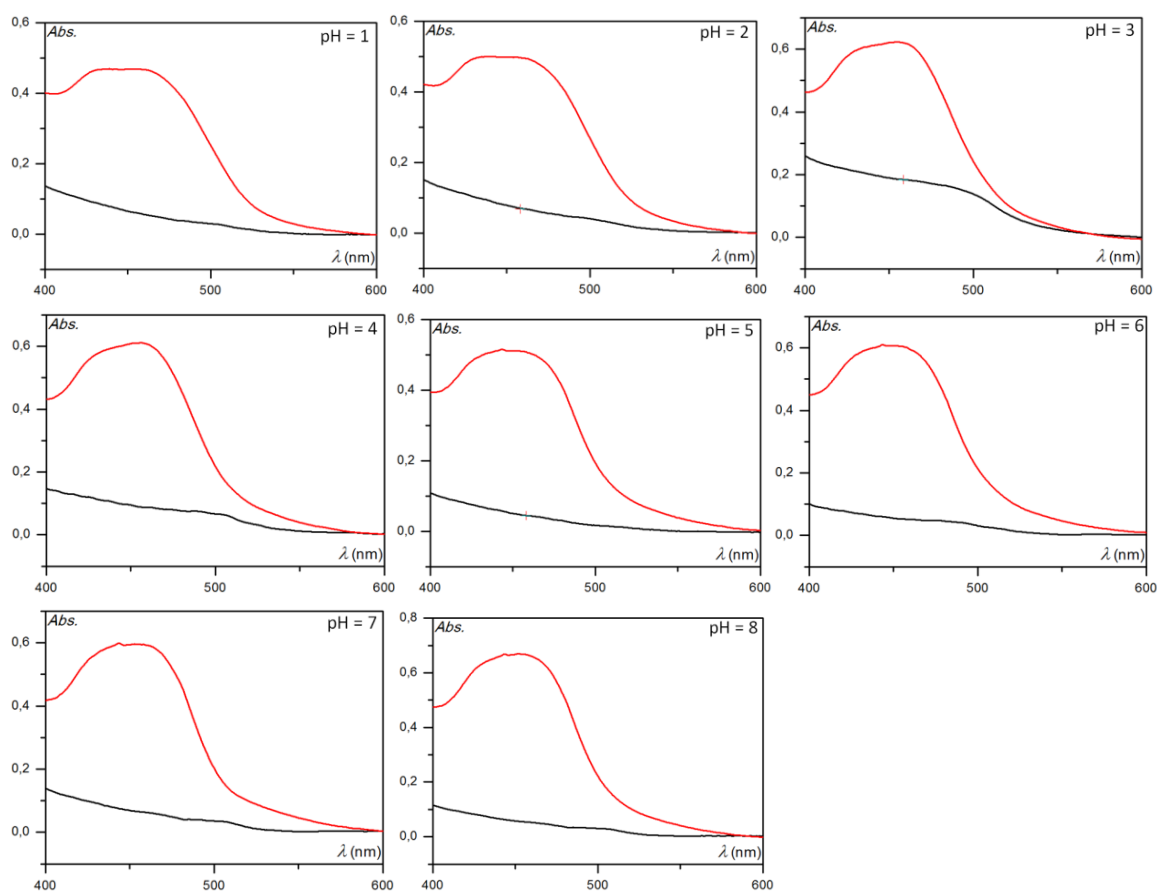


Figure S11. UV-vis absorption spectra of RuAc/TiO₂/FTO before (*red*) and after (*black*) 80 min photoelectrooxidation of 0.5 M NaClO₄ aqueous solutions at specified pH.

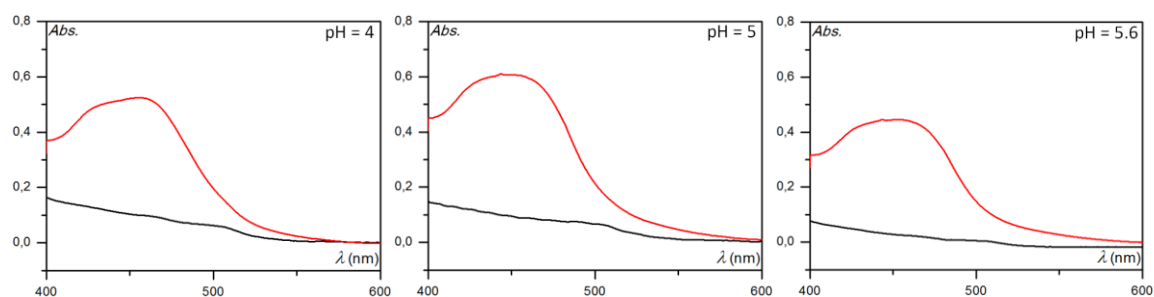


Figure S12. UV-vis absorption spectra of RuAc/TiO₂/FTO before (*red*) and after (*black*) 80 min photoelectrooxidation of 0.1 M acetate buffer at specified pH.

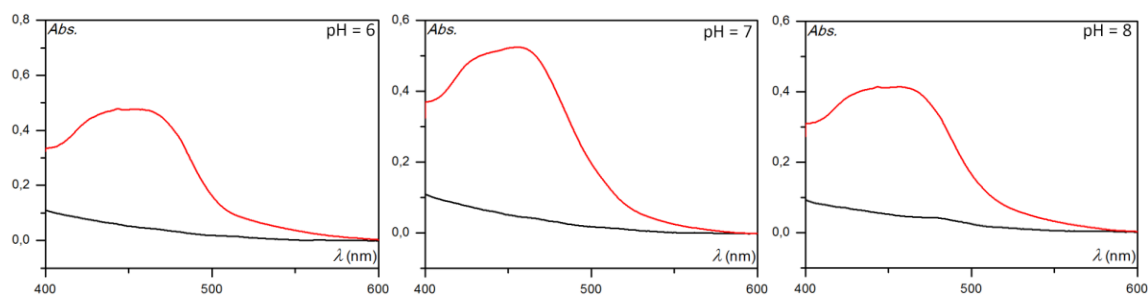


Figure S13. UV-vis absorption spectra of RuAc/TiO₂/FTO before (*red*) and after (*black*) 80 min photoelectrooxidation of 0.1 M phosphate buffer at specified pH.

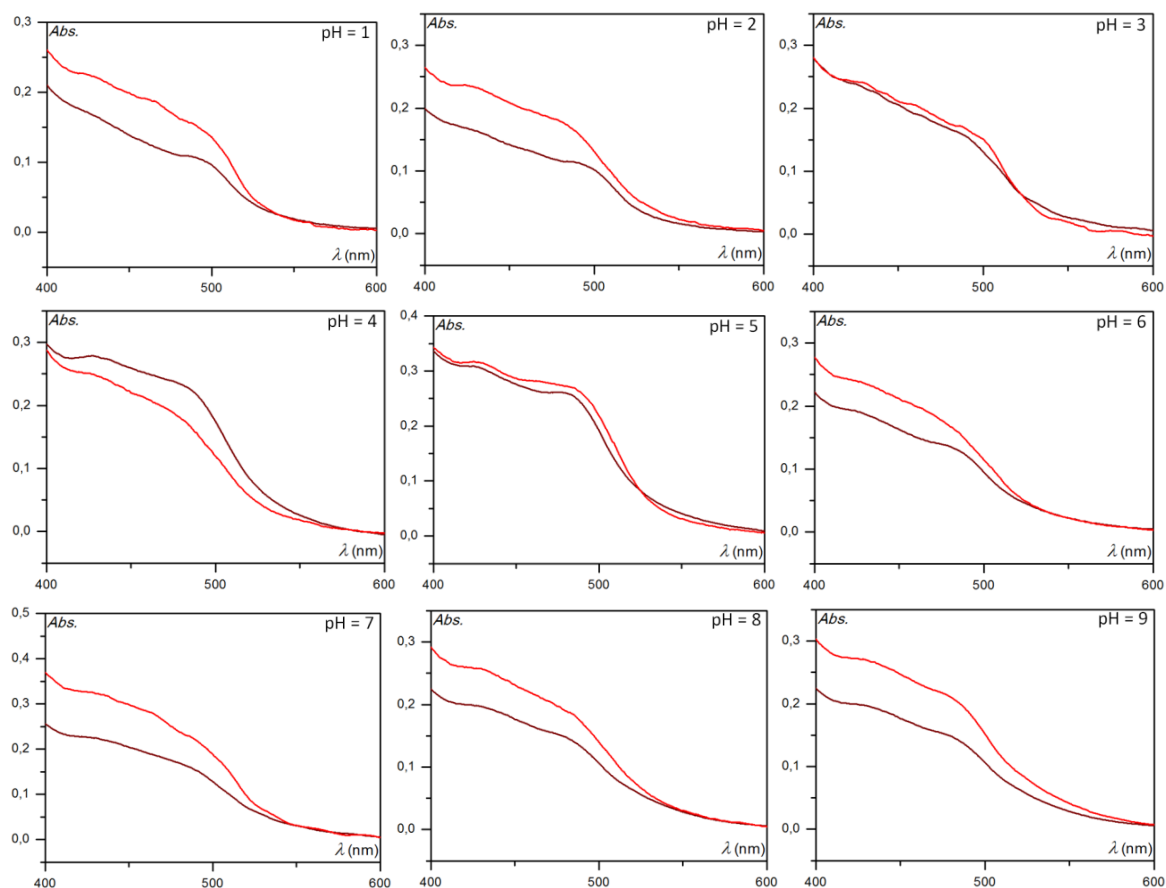


Figure S14. UV-vis absorption spectra of RuNPhSiSi/TiO₂/FTO before (*red*) and after (*brown*) 80 min photoelectrooxidation of 0.5 M NaClO₄ aqueous solution at specified pH.

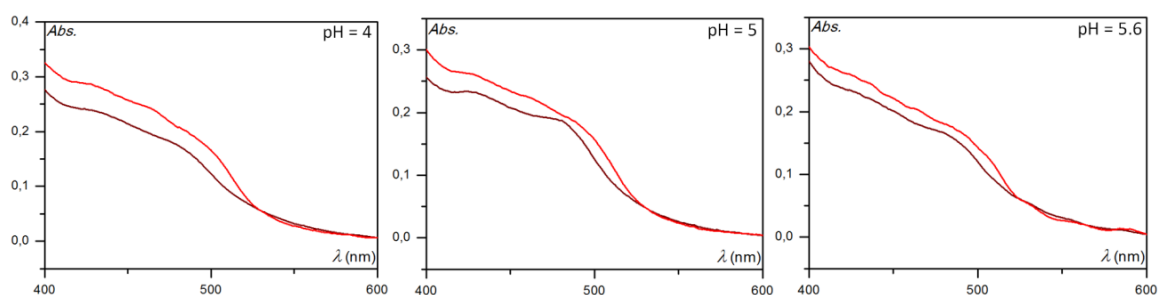


Figure S15. UV-vis absorption spectra of RuNPhSiSi/TiO₂/FTO before (*red*) and after (*brown*) 80 min photoelectrooxidation of 0.1 M acetate buffer at specified pH.

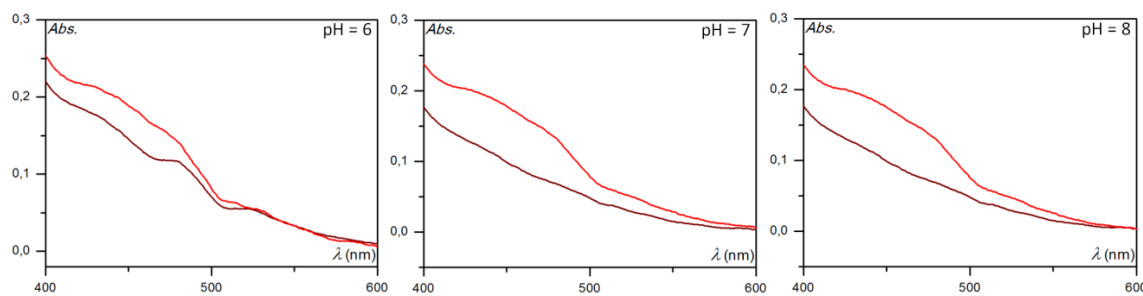


Figure S16. UV-vis absorption spectra of RuNPhSiSi/TiO₂/FTO before (*red*) and after (*black*) 80 min photoelectrooxidation of 0.1 M phosphate buffer at specified pH.

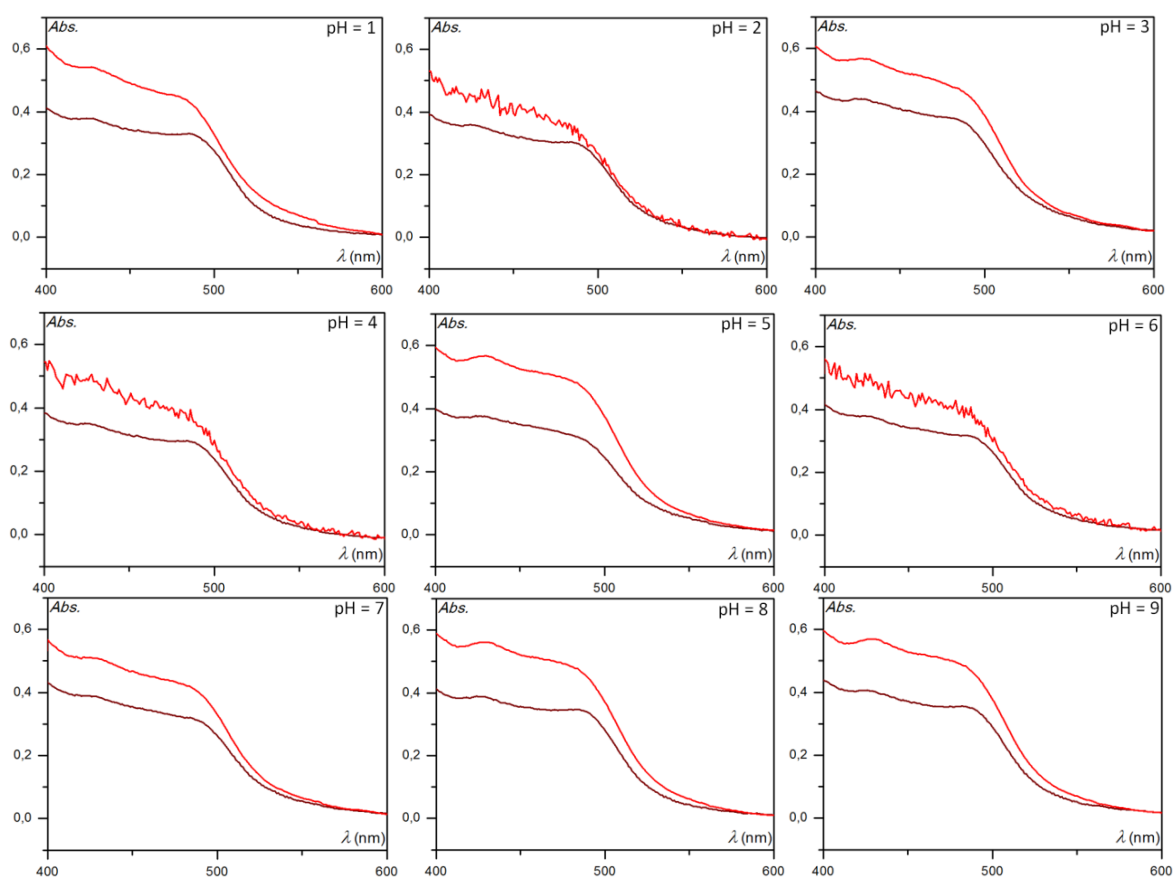


Figure S17. UV-vis absorption spectra of RuNPhAcSi/TiO₂/FTO before (red) and after (brown) 80 min photoelectrooxidation of 0.5 M NaClO₄ aqueous solution at specified pH.

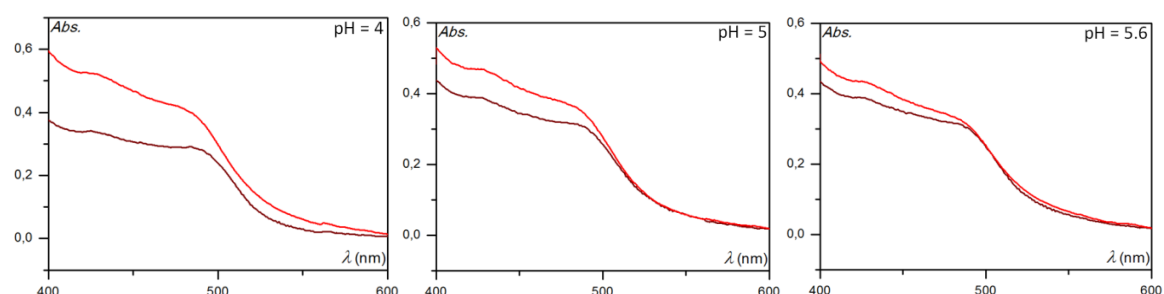


Figure S18. UV-vis absorption spectra of RuNPhAcSi/TiO₂/FTO before (red) and after (brown) 80 min photoelectrooxidation of 0.1 M acetate buffer at specified pH.

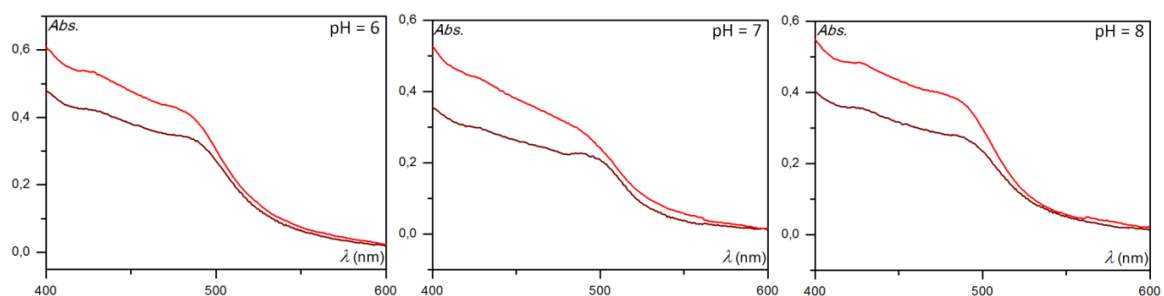


Figure S19. UV-vis absorption spectra of RuNPhAcSi/TiO₂/FTO before (red) and after (brown) 80 min photoelectrooxidation of 0.1 M phosphate buffer at specified pH.

SUPPLEMENTARY REFERENCES

- (S1) N. Connelly, T. Damhus, R. Hartshorn, A. Hutton, *Parent Hydride Names and Substitutive Nomenclature. In Nomenclature of Inorganic Chemistry: IUPAC Recommendations 2005*; **2005**; 107.
- (S2) G. P. Moss, P. A. S. Smith, D. Tavernier, *Pure Appl. Chem.* 1995, **67**, 1307.
- (S3) D. L. Ashford, M. K. Gish, A. K. Vannucci, M. K. Brennaman, J. L. Templeton, J. M. Papanikolas, T. J. Meyer, *Chem. Rev.* 2015, **115**, 13006.
- (S4) M. K. Brennaman, R. J. Dillon, L. Alibabaei, M. K. Gish, C. J. Dares, D. L. Ashford, R. L. House, G. J. Meyer, J. M. Papanikolas, T. J. Meyer, *J. Am. Chem. Soc.* 2016, **138**, 13085.
- (S5) Z. Yu, F. Li, L. Sun, *Energy Environ. Sci.* 2015, **8**, 760.
- (S6) P. Xu, N. S. McCool, T. E. Mallouk, *Nano Today* 2017, **14**, 42.
- (S7) E. A. Gibson, *Chem. Soc. Rev.*, 2017, **46**, 6194-6209.
- (S8) E. Terpetschnig, H. Szmecinski, H. Malak, J. R. Lakowicz, *Biophys. J.* 1995, **68**, 342.
- (S9) P. D. Beer, F. Szemes, V. Balzani, C. M. Sala, M. G. B. Drew, S. W. Dent, M. Maestri, *J. Am. Chem. Soc.* 1997, **119**, 11864.